Fermilab

Fermi National Accelerator Laboratory
P.O. Box 500 • Batavia, Illinois • 60510

TD-97-054
December 1, 1997
Rev July 28, 1998

HGQ Magnetic Shim Performance

G. Sabbi

1 Introduction

Fermilab, Lawrence Berkeley National Laboratory and Brookhaven National Laboratory have formed a consortium to provide components for the Large Hadron Collider (LHC) to be built at CERN. The U.S. contribution includes half of the high gradient quadrupoles (HGQ) for the inner focusing triplets. These magnets must provide a field gradient of 200 T/m over a 70 mm bore, with a sufficient margin in order to withstand the heavy heat load due to secondary particles from beam-beam collisions [1]. At the same time, due to large and rapidly varying values of the β-function, a high field quality is required [2].

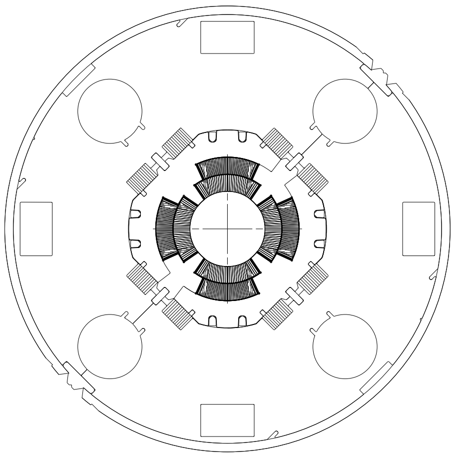

Figure 1: HGQ cross-section.

The HGQ design [3] incorporates magnetic shims for correction of low-order non-allowed harmonics generated by random conductor positioning errors. The HGQ cross section is shown in Figure 1. The tuning shims are housed in eight rectangular gaps between collars and yoke. The iron yoke contributes about 10% of the central field. Its inner radius at the midplane is 92.56 mm; the outer radius is 200 mm.

2 Definitions

The following conventions shall be adopted. The magnet axis is chosen as the z axis of a cylindrical coordinate system. The positive z direction goes from the magnet lead end towards the return end. The azimuthal coordinate increases counterclockwise when seen from the positive z axis. The reference azimuth $\theta = 0$ is at the boundary between quadrant 1 and 4, as labelled during magnet production [4]. With this definition, quadrant 1 occupies the sector $0 < \theta < \pi/2$, quadrant 2 is in the sector $\pi/2 < \theta < \pi$, etc. On top of the cylindrical coordinate system, a cartesian system is defined with same z axis, x axis at θ=0, y axis at $\theta = \pi/2$. The magnet is powered so to provide a current flow in the negative z direction in the octants which depart from the horizontal (x) mid-plane, in the positive z direction in the octants which depart from the vertical (y) mid-plane. The octants are labelled according to the quadrant in which they are located and the direction of the current flow: octant 1N for quadrant 1, negative current flow ($0 < \theta < \pi/4$); octant 1P for quadrant 1, positive current flow ($\pi/4 < \theta < \pi/2$); and so forth. The tuning shims are named after the octant to which they belong. In the nominal position, each tuning shim cavity is filled with 1 cm of iron laminations on the midplane side, the remaining part being filled with nonmagnetic laminations. A general position is then given in terms of a filling parameter f, which specifies the thickness [mm] of iron laminations added ($f > 0$) or removed ($f < 0$) with respect to the nominal position (f=0). The allowed range of variation for the f parameter is $-10 < f < 10$.

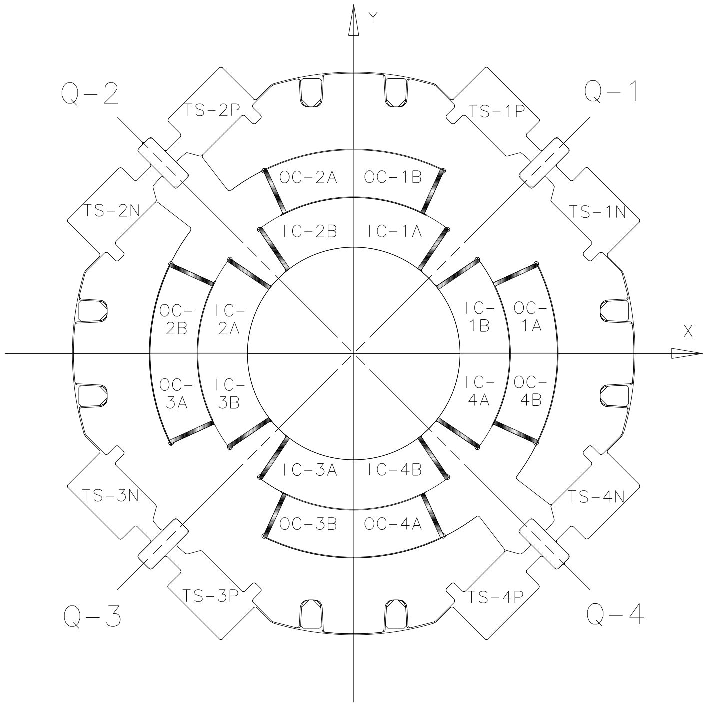

Figure 2: HGQ collared coil cross-section (view from return end).

3 Field representation

In the straight section of the magnet, where translational symmetry applies and the longitudinal component of the magnetic field vanishes, the magnetic field in the bore can be represented in terms of multipole coefficients defined according to the following expression:

$$\begin{aligned} B_\theta(r,\theta) &= \sum_{n=1}^{\infty} \left(\frac{r}{r_0}\right)^{n-1} (B_n \cos n\theta - A_n \sin n\theta) \\ B_r(r,\theta) &= \sum_{n=1}^{\infty} \left(\frac{r}{r_0}\right)^{n-1} (A_n \cos n\theta + B_n \sin n\theta) \end{aligned}$$

With the definitions in section 2, the main field component B_2 is positive, and the quadrupole magnet will horizontally focus and vertically defocus a positive charged beam travelling in the positive z direction. The same multipole coefficients appear in the equivalent expansion in complex notation:

$$B_y(x,y) + iB_x(x,y) = \sum_{n=1}^{\infty} (B_n + iA_n) \left(\frac{x+iy}{r_0}\right)^{n-1} \tag{1}$$

As customary for LHC magnets, the harmonics will be expressed in "units" of 10^{-4} of the main field component at a reference radius of 1 cm:

$$b_n = B_n/B_2 \cdot 10^4 \qquad a_n = A_n/B_2 \cdot 10^4$$

4 Computer Model

Since the eight magnetic shims are operated independently, the 8-fold symmetry of the magnet cross-section is broken, and it is necessary to define a 360 degrees model. This model can be used to compute the effect on the harmonics due to any shim configuration, as compared to the nominal case. However, in practice it is only necessary to compute the field change as function of the position of a single shim, when all the others are kept in the nominal position. The effect of each of the other shims can then be obtained based on symmetry considerations, and the effect of a general shim configuration can be computed by linear addition. In fact, since the contribution of each tuning shim represents a small perturbation with respect to the main quadrupole field, they can be treated as independent effects.

The analysis has been carried out using the POISOPT optimization routine [5] interfaced to the POISSON package [6, 7]. POISOPT allows to define a parametrized model in which the geometrical dimensions of the various features (coil block angles, yoke radii, cooling holes, busbar cavity) can be easily modified either by the user or by an optimization routine. In particular, 8 parameters control the tuning shim configuration. In order to simplify the geometry definition, the inner region of the model is horizontally split in two halves.

The HGQ cross-section model is shown in Figure 3. In this example, the tuning shim configuration allows a b_3 correction of -5 units at I=14 kA.

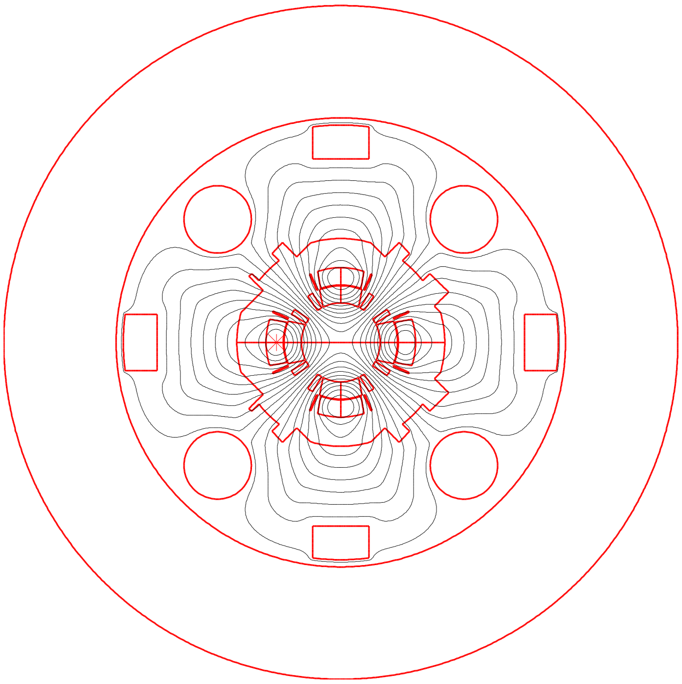

Figure 3: HGQ cross-section model and contour lines of the vector potential at 14 kA for a tuning shim configuration designed to provide a b_3 correction of -5 units.

5 Harmonics generated by tuning shim 1N

Table 1-6 show the variation in normal and skew multipole components of order 1 to 6 as function of the position of tuning shim 1N. Due to saturation effects, the correction depends on current. For each component, the values corresponding to an excitation current of 0.8 kA, 11.1 kA and 13.9 kA (i.e. injection, operating gradient and maximum gradient [8]) are given.

Table 7 shows, for each multipole order, a comparison between the harmonic correction allowed by a single tuning shim at nominal gradient, the expected RMS spread of the magnet errors before shimming, and the expected systematic measurement errors [9]. As can be seen, for increasing multipole orders the tuning shim correction capability is decreasing relative to the expected magnet and measurement errors. Based on this result, it is not expected that the tuning shim correction scheme can provide significant improvements of the HGQ field quality for $n > 4$. The sextupole and octupole corrections as function of the position of tuning shim 1N for an excitation current of 11.1 kA are plotted in Figure 4 and 5.

Table 1: Variation in the normal and skew dipole as function of the position of shim 1N.

f	Δb_1			Δa_1		
[mm]	I=0.8 kA	I=11.1 kA	I=13.9 kA	I=0.8 kA	I=11.1 kA	I=13.9 kA
-10.0	-34.2118	-23.7051	-16.4956	-67.4538	-43.3638	-32.3022
-7.5	-26.9933	-18.4998	-12.4098	-51.7705	-32.8501	-24.2020
-5.0	-18.8189	-12.8068	-8.1927	-35.1650	-22.1583	-16.1848
-2.5	-9.4106	-6.6953	-4.1511	-17.5458	-11.1206	-8.1259
.0	.0000	.0000	.0000	.0000	.0000	.0000
2.5	10.6973	7.0387	4.2506	17.8715	11.3487	7.9021
5.0	21.9580	14.4758	8.8228	35.7511	23.0698	15.5516
7.5	34.0170	21.9280	13.4335	53.5764	34.7999	23.1351
10.0	46.6803	30.2933	18.2611	71.0194	45.4335	30.5151

Table 2: Variation in the normal and skew quadrupole as function of the position of shim 1N.

f	Δb_2			Δa_2		
[mm]	I=0.8 kA	I=11.1 kA	I=13.9 kA	I=0.8 kA	I=11.1 kA	I=13.9 kA
-10.0	-1.9607	-17.4165	-16.0265	-9.8015	-5.2550	-3.9234
-7.5	-1.5415	-13.5577	-12.1617	-7.3397	-3.9331	-2.9519
-5.0	-1.0729	-9.2733	-8.2088	-4.8383	-2.6035	-1.9836
-2.5	-.5545	-4.7803	-4.1223	-2.3593	-1.2686	-.9813
.0	.0000	.0000	.0000	.0000	.0000	.0000
2.5	.5899	5.0735	4.2295	2.2142	1.2186	.9012
5.0	1.2098	10.2448	8.5735	4.2176	2.3421	1.7084
7.5	1.8588	15.6713	13.0010	6.0035	3.4023	2.4463
10.0	2.5281	21.0834	17.5047	7.5213	4.2607	3.1020

Table 3: Variation in the normal and skew sextupole as function of the position of shim 1N.

f	Δb_3			Δa_3		
[mm]	I=0.8 kA	I=11.1 kA	I=13.9 kA	I=0.8 kA	I=11.1 kA	I=13.9 kA
-10.0	-2.6758	-1.5706	-1.1832	-.4384	-.0430	-.0040
-7.5	-2.0846	-1.2075	-.9065	-.2682	-.0008	.0057
-5.0	-1.4373	-.8274	-.6167	-.1376	.0237	.0099
-2.5	-.7341	-.4229	-.3114	-.0380	.0233	.0109
.0	.0000	.0000	.0000	.0000	.0000	.0000
2.5	.7599	.4392	.3128	-.0171	-.0526	-.0305
5.0	1.5338	.8851	.6248	-.1149	-.1320	-.0828
7.5	2.3105	1.3368	.9349	-.2821	-.2509	-.1554
10.0	3.0702	1.7695	1.2416	-.5216	-.3886	-.2491

Table 4: Variation in the normal and skew octupole as function of the position of shim 1N.

f	Δb_4			Δa_4		
[mm]	I=0.8 kA	I=11.1 kA	I=13.9 kA	I=0.8 kA	I=11.1 kA	I=13.9 kA
-10.0	-.3766	-.1913	-.1453	.1186	.1025	.0873
-7.5	-.2887	-.1457	-.1110	.1054	.0841	.0697
-5.0	-.1967	-.0986	-.0748	.0825	.0620	.0494
-2.5	-.0984	-.0490	-.0368	.0467	.0337	.0262
.0	.0000	.0000	.0000	.0000	.0000	.0000
2.5	.0928	.0493	.0361	-.0595	-.0398	-.0298
5.0	.1815	.0961	.0691	-.1318	-.0855	-.0630
7.5	.2635	.1400	.1006	-.2167	-.1361	-.0995
10.0	.3352	.1786	.1293	-.3122	-.1893	-.1392

Table 5: Variation in the normal and skew decapole as function of the position of shim 1N.

f	Δb_5			Δa_5		
[mm]	I=0.8 kA	I=11.1 kA	I=13.9 kA	I=0.8 kA	I=11.1 kA	I=13.9 kA
-10.0	-.0378	-.0164	-.0115	.0377	.0220	.0175
-7.5	-.0278	-.0120	-.0085	.0311	.0176	.0140
-5.0	-.0178	-.0076	-.0055	.0229	.0126	.0099
-2.5	-.0083	-.0036	-.0026	.0122	.0067	.0052
.0	.0000	.0000	.0000	.0000	.0000	.0000
2.5	.0070	.0030	.0021	-.0138	-.0074	-.0057
5.0	.0122	.0051	.0036	-.0290	-.0154	-.0117
7.5	.0149	.0064	.0045	-.0449	-.0240	-.0179
10.0	.0151	.0068	.0047	-.0620	-.0325	-.0244

Table 6: Variation in the normal and skew dodecapole as function of the position of shim 1N.

f	Δb_6			Δa_6		
[mm]	I=0.8 kA	I=11.1 kA	I=13.9 kA	I=0.8 kA	I=11.1 kA	I=13.9 kA
-10.0	-.0019	-.0004	-.0002	.0066	.0033	.0026
-7.5	-.0011	-.0001	-.0001	.0053	.0026	.0021
-5.0	-.0005	.0001	.0000	.0038	.0019	.0015
-2.5	-.0002	.0001	.0001	.0020	.0010	.0008
.0	.0000	.0000	.0000	.0000	.0000	.0000
2.5	-.0002	-.0001	-.0001	-.0020	-.0009	-.0007
5.0	-.0008	-.0003	-.0004	-.0041	-.0020	-.0014
7.5	-.0018	-.0008	-.0008	-.0061	-.0029	-.0022
10.0	-.0032	-.0014	-.0012	-.0080	-.0039	-.0029

Table 7: comparison between the correction allowed by a tuning shim, the expected RMS spread of the magnet errors before shimming, and the expected systematic measurement errors.

n	Shim correction	Magnet RMS spread	Measurement systematic
3	1.5	1.3	0.16
4	0.2	0.4	0.08
5	0.02	0.09	0.04
6	0.001	0.03	0.02

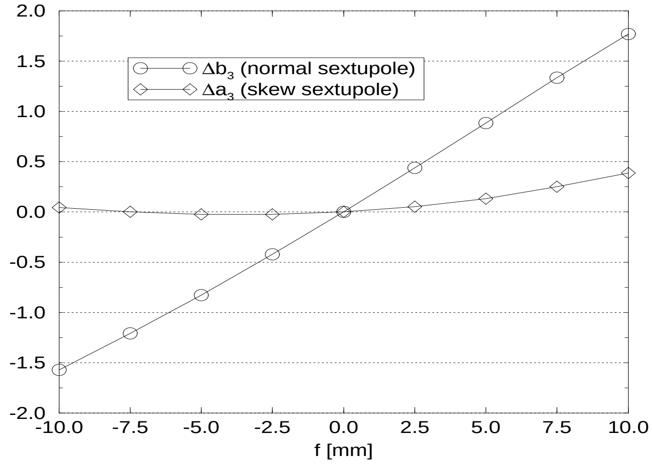

Figure 4: Normal and skew sextupole correction as function of the position of tuning shim 1N at I=11.1 kA (all other shims are kept in nominal position, $f = 0$.

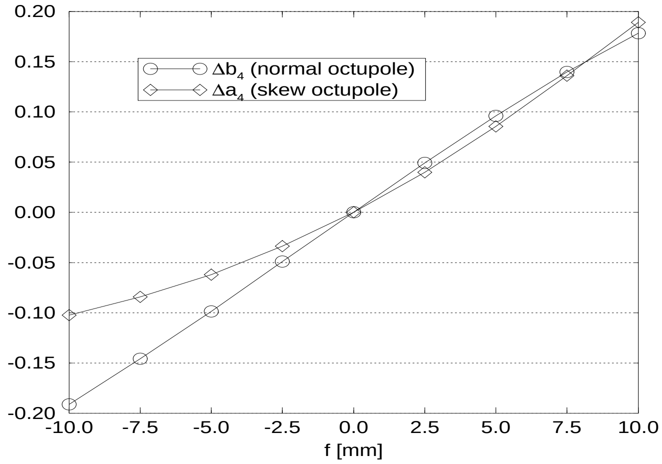

Figure 5: Normal and skew octupole correction as function of the position of tuning shim 1N at I=11.1 kA (all other shims are kept in nominal position, $f = 0$.

6 Symmetries in the harmonics generated by tuning shims

If the harmonics generated by tuning shim 1N are know, then the harmonics generated by the other tuning shims can be obtained based on symmetry operations. The basic tranformations which are needed are a rotation of the reference frame by an angle $\pi/2$, a reflection of the reference frame with respect to the x axis and an inversion of the current flow. Table 8 shows how the multipole coefficients are transformed when one of these basic symmetry operations is applied. For details of how these relations are derived, see Ref. [10].

Table 8: Harmonic tranformations following a symmetry operation. B'_n, A'_n indicate the multipole components computed after the symmetry operation. B_n, A_n indicate the multipole components computed before the symmetry operation, which are supposed to be known. Note the rotations/reflections are meant to be applied to the reference frame, not to the physical system.

Symmetry operation	$n = 2k-1$		$n = 2k$	
	B'_n	A'_n	B'_n	A'_n
Identity	B_n	A_n	B_n	A_n
Rot. $\pi/2$	$(-1)^k A_n$	$(-1)^{k+1} B_n$	$(-1)^k B_n$	$(-1)^k A_n$
Rot. π	$-B_n$	$-A_n$	B_n	A_n
Rot. $3\pi/2$	$(-1)^{k+1} A_n$	$(-1)^k B_n$	$(-1)^k B_n$	$(-1)^k A_n$
Refl. x axis	-B_n	A_n	$-B_n$	A_n
Pol. switch	-B_n	$-A_n$	-B_n	$-A_n$

Table 9: Symmetry tranformations which give the harmonics for shim 2P, 3N, 4P starting from shim 1N configurations and for shim 2N, 3P, 4N starting from shim 1P configurations. Note the rotations are meant to be applied to the reference frame, not to the physical system.

Shim	Rot. angle	Polarity switch	Shim	Rot. angle	Polarity switch
1N	0	No	1P	0	No
2P	$3\pi/2$	Yes	2N	$3\pi/2$	Yes
3N	$2(\pi/2)$	No	3P	$2(\pi/2)$	No
4P	$(\pi/2)$	Yes	4N	$(\pi/2)$	Yes

Table 9 shows the symmetry operations which have to be applied in order to obtain the configurations in which each of tuning shims 2P, 3N, 4P is independently operated, starting by the 1N configurations analyzed in section 5, and the corresponding symmetry operations which have to be applied in order to obtain the configurations in which each of tuning shims 2N, 3P, 4N is independently operated, starting by the 1P configurations.

The harmonics generated by shim 1P can be obtained from the 1N configurations by applying a reflection with respect to the bysectrix of quadrant 1-3. This transformation is illustrated in Figure

6: it can be obtained by combining a reflection of the reference frame with respect to the X axis followed by a rotation of the reference frame by $\pi/2$. Despite of the fact that the current flows in the 1P octant in the opposite direction with respect to the 1N octant, a polarity switch should *not* be applied: this feature is already included in the transformation since the Z axis changes orientation in the reflected reference frame.

Finally, table 10 shows the symmetry relations between the harmonics generated by the different tuning shims. Since the main field component B_2 is invariant for each of the resulting transformations the same relations hold for the *multipole coefficients expressed in "units"*.

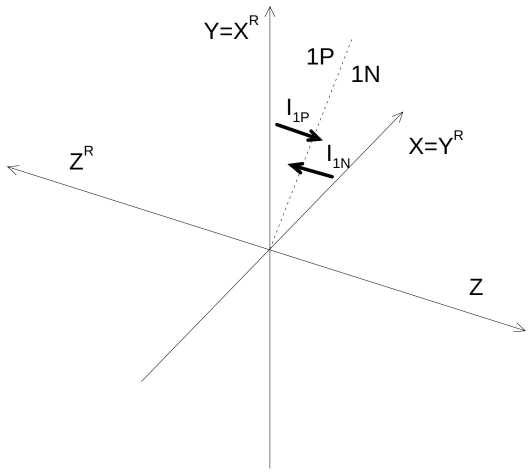

Figure 6: Coordinate transformation for reflection with respect to the bysectrix of quadrant 1-3.

Table 10: Symmetries in the harmonics generated by tuning shims. B'_n, A'_n indicate the multipole components computed for each tuning shim. B_n, A_n indicate the multipole components computed for shim 1N, which are given in Table 1-6.

Magnetic shim	$n = 2k-1$		$n = 2k$	
	B'_n	A'_n	B'_n	A'_n
1N	B_n	A_n	B_n	A_n
1P	$(-1)^{k+1}A_n$	$(-1)^{k+1}B_n$	$(-1)^{k+1}B_n$	$(-1)^{k}A_n$
2P	$(-1)^{k}A_n$	$(-1)^{k+1}B_n$	$(-1)^{k+1}B_n$	$(-1)^{k+1}A_n$
2N	$-B_n$	A_n	B_n	$-A_n$
3N	$-B_n$	$-A_n$	B_n	A_n
3P	$(-1)^{k}A_n$	$(-1)^{k}B_n$	$(-1)^{k+1}B_n$	$(-1)^{k}A_n$
4P	$(-1)^{k+1}A_n$	$(-1)^{k}B_n$	$(-1)^{k+1}B_n$	$(-1)^{k+1}A_n$
4N	B_n	$-A_n$	B_n	$-A_n$

7 Conclusions

Calculations of the change in the multipole field components as function of the HGQ tuning shim configuration have been presented. These results will be validated by comparison with magnetic measurements during the HGQ model magnet program. For increasing multipole orders the tuning shim correction capability is decreasing relative to the expected magnet and measurement errors. Based on this result, it is not expected that the tuning shim correction scheme can provide an effective correction of the HGQ multipole errors for $n > 4$.

References

[1] R. Ostojic, T. Taylor, S. Weisz, "Systems Layout of the Low-β Insertions for the LHC Experiments", 1997 Particle Accelerator Conference, Vancouver, Canada, May 1997.

[2] A. Faus-Golfe, A. Verdier, "Dynamic Aperture Limitations of the LHC in Physics Conditions due to Low-β Insertions", Proc. European Particle Accelerator Conference, June 1996.

[3] R. Bossert et al., "Development of a High Gradient Quadrupole for the LHC Interaction Regions", 1996 Applied Superconducivity Conference, Pittsburgh, August 1996.

[4] High Gradient Quadrupole Coil Insulation/Assembly Reference Drawing (5520-MD-344376).

[5] S. Russenschuck, T. Tortschanoff, "Mathematical optimization of superconducting accelerator magnets", CERN AT/93-37 (MA), May 1994.

[6] F. Rohner, "User Guide of the Cern-Poisson program package", May 1992.

[7] R. Holsinger, C. Iselin, "The Cern-Poisson package user guide", Cern Program Library long writeup, August 1984.

[8] G. Sabbi, J. Strait, A. Zlobin, S. Caspi, "Magnetic Field Analysis of the First Short Models of a High Gradient Quadrupole for the LHC Interaction Regions", 15th International Conference on Magnet Technology, Beijing, China, October 1997.

[9] G. Sabbi et al., "Magnetic Design of a High-Gradient Quadrupole for the LHC low-β Insertions", 1997 Particle Accelerator Conference, Vancouver, Canada, May 1997.

[10] G. Sabbi, "Coordinate Transformations of Harmonic Field Components", Fermilab TD-97-053, November 1997.